

THE INCORPORATION OF ALKALIS IN BERYL: MULTI-NUCLEAR MAS NMR AND CRYSTAL-STRUCTURE STUDY

BARBARA L. SHERRIFF* AND H. DOUGLAS GRUNDY

Department of Geology, McMaster University, Hamilton, Ontario L8S 4M1

J. STEPHEN HARTMAN

Department of Chemistry, Brock University, St. Catharines, Ontario L2S 3A1

FRANK C. HAWTHORNE AND PETR ČERNÝ

Department of Geological Sciences, University of Manitoba, Winnipeg, Manitoba R3T 2N2

ABSTRACT

The stereochemical details of the incorporation of alkali ions into the beryl structure are examined by multi-nuclear MAS NMR spectroscopy and single-crystal structure refinement. The ^{29}Si signal is narrow in alkali-poor beryl, and broadens with increasing alkali content, a result of the different short-range next-nearest-neighbor configurations produced by the incorporation of alkalis into the structure; we designate this substitutional broadening, and calculate its value from the proposed local configurations and the method of Sherriff & Grundy (1988). Substitutional broadening is observed in the ^{27}Al spectra that also show only [6]-coordinate Al to be present, in agreement with the current and earlier X-ray results. Two ^7Li signals are observed, indicating that Li occurs both as a framework constituent and as a channel species. The crystal structures of the four samples were refined, to R indices of 2-3% using $\text{MoK}\alpha$ X radiation. The $\langle \text{Be-O} \rangle$ distance expands linearly with increasing Li \Rightarrow Be substitution at this site, but the O-Be-O bond angles remain unchanged. This substitution produces a bond-valence deficiency at the O(2) anion. This is compensated by lengthening of Si-O(1) and Si-O(1)a, and contraction of Si-O(2) with increasing Li \Rightarrow Be substitution. All samples of alkali-bearing beryl examined show residual electron density in the channels due to occupancy by alkali ions; all show more density at the 2a site than at the 2b site. Comparison of these residual densities with known alkali contents confirms previous work that assigned Cs to the 2a position. The electron density observed at the 2b position correlates well with the Na contents and is insufficient to account for the H_2O ; thus we assign Na to 2b and H_2O to 2a. Local stereochemistry and analytical results suggest that Na is bonded to two H_2O groups in the channel.

Keywords: beryl, alkali-rich beryl, nuclear magnetic resonance, magic angle spinning, structure refinements.

SOMMAIRE

Nous examinons les détails stéréochimiques concernant l'incorporation des alcalins dans la structure du béryl au moyen de la résonance magnétique nucléaire avec spin selon

l'angle magique et de l'affinement de la structure de cristaux uniques. Le signal de ^{29}Si est étroit dans le béryl à faible teneur en alcalin, et devient plus large avec une augmentation en teneur d'alcalin, résultat des configurations différentes à courte échelle parmi les atomes immédiatement avoisinants que cause l'incorporation des alcalins dans la structure. Nous désignons ce phénomène *élargissement substitutionnel*, et calculons sa valeur à partir des schémas locaux proposés et la méthode de Sherriff et Grundy (1988). Un élargissement substitutionnel est aussi présent dans les spectres de ^{27}Al , qui font preuve de la seule présence de $^{\text{VI}}\text{Al}$, en concordance avec nos résultats de diffraction X et les travaux antérieurs. Nous trouvons deux signaux pour ^7Li , ce qui fait penser que le Li joue deux rôles, faisant partie de la trame et aussi situé dans les canaux. Nous avons affiné la structure cristalline de quatre échantillons, jusqu'à des indices R de 2-3% en utilisant un rayonnement $\text{MoK}\alpha$. La distance $\langle \text{Be-O} \rangle$ augmente de façon linéaire à mesure que le Li remplace le Be, mais l'angle O-Be-O demeure inchangé. Cette substitution produit un déficit dans la valence de liaison sur l'atome O(2), qui est compensé par une augmentation de la longueur de Si-O(1) et Si-O(1)a, et une contraction dans Si-O(2) qui dépend de l'importance de la substitution du Li au Be. Tout béryl qui contient des alcalins montre une densité des électrons résiduelle dans les canaux à cause de la présence des alcalins; tous les échantillons étudiés font preuve de plus de densité électronique sur le site 2a que sur le site 2b. Une comparaison des densités résiduelles avec les teneurs spécifiques des éléments confirme les conclusions antérieures qui attribuent au Cs la position 2a. La densité des électrons au site 2b concorde bien avec l'attribution du Na à cette position, et ne suffit pas pour y expliquer la présence de H_2O . Nous attribuons donc le Na à 2b, et le H_2O à 2a. Les considérations de stéréochimie locale et les résultats analytiques nous poussent à croire que le Na est associé à deux groupes H_2O dans les canaux.

(Traduit par la Rédaction)

Mots-clés: béryl, béryl enrichi en alcalins, résonance magnétique nucléaire, spin selon l'angle magique, affinement de la structure.

INTRODUCTION

Beryl is a common constituent of granitic pegma-

*Present address: Department of Geological Sciences, University of Manitoba, Winnipeg, Manitoba R3T 2N2.

tites, and its compositional variation correlates strongly with the geochemical and paragenetic characteristics of the pegmatites in which it occurs (Beus 1960, Černý 1975). Of particular significance in this regard is the substitution of alkalis into the structure. Beryl consists of a $[\text{Be}_3\text{Al}_2\text{Si}_6\text{O}_{18}]$ framework (Zoltai 1960, Hawthorne & Smith 1986) with prominent channels parallel to the *Z* axis. Possible substitution of Be by Li into the framework tetrahedra introduces a charge deficiency that is compensated by the incorporation of alkalis into the large channels (which also usually contain significant amounts of H_2O). Details of the alkali contents are particularly useful in the identification of petrogenetically related pegmatites (Černý 1975) and in the estimation of degree of fractionation of their host pegmatite (Černý 1989). In view of the petrological importance of alkali-bearing beryl, together with its intrinsic crystal-chemical interest, a detailed understanding of these schemes of substitution is desirable to distinguish between crystal-chemical and geochemical influences on bulk composition of the mineral.

The structure of beryl was solved by Bragg & West (1926); Gibbs *et al.* (1968) and Morosin (1972) gave refinements of synthetic beryl. Refinements of crystals of alkali-bearing beryl are reported by Bakakin *et al.* (1969), Hawthorne & Černý (1977), Brown & Mills (1986) and Aurisicchio *et al.* (1988). Although several samples of alkali-bearing beryl have been examined in previous studies, they are all of approximately the same Li content. In order to elucidate the mechanisms of substitution, a range of compositions is desirable; the samples of the present study were selected on this basis. Details of the average structure are derived from crystal-structure refinement, and details of local structure are probed by multi-nuclear MAS NMR (Magic-Angle Spinning Nuclear Magnetic Resonance).

SAMPLES

Four samples of alkali-bearing beryl from granitic pegmatites in Manitoba were used in this work: SHEE-1-6 from Shatford Lake, and EEE-10, BLM-503 and T-24 from the Tanco pegmatite. These were supplemented by two samples of emerald from New South Wales and Colombia (Ottaway *et al.* 1986).

Beryl SHEE-1-6 comes from the SHEE-1 pegmatite dike at the eastern end of Shatford Lake, southeastern Manitoba. The dike belongs to the Shatford Lake Group, enriched in Nb, Y, REE, Ti, Be, F, (Zr, U, Th) and classified as a gadolinite subtype of rare-element granitic pegmatites (Černý *et al.* 1981). This pegmatite group is related to an A-type, metaluminous, sheared and foliated-to-lined

leucogranite that forms the eastern extremity of the Lac du Bonnet batholith (Černý *et al.* 1987). The beryl is greenish yellow, columnar (1×3 cm), and is associated with microcline perthite, quartz and accessory garnet in the blocky core of the pegmatite.

Samples EEE-10, BLM-503 and T-24 were collected in the Tanco pegmatite at Bernic Lake, southeastern Manitoba. This pegmatite is a classic representative of the complex-type, petalite subtype rare-element granitic pegmatite, with substantial lepidolite and amblygonite-montebrazite (Černý 1982). Tanco belongs to the Bernic Lake group of closely related pegmatites. Its parent granite is not exposed at the present erosional surface, but is presumed (by analogy with broadly similar groups of granitic pegmatites in the region) to be strongly peraluminous, and garnet- and muscovite-bearing (Černý *et al.* 1981).

Beryl EEE-10 is typical of albitic unit (3) in the eastern extremity of the pegmatite, where it occurs in white to pink columnar crystals (1×3 to 4×15 cm) associated with saccharoidal albite and albite of the cleavelandite habit, quartz, abundant black tourmaline and minor oxide minerals of Ta. Sample EEE-10 is brownish pink, cloudy to gemmy, $4 \times 6 \times 10$ cm in size, and anhedral along the contact with albite and minor muscovite.

Sample BLM-503 is a white, milky-to-transparent, short prismatic crystal, 2×3 cm in size. It is in part euhedral against quartz, in part anhedral along the contact with microcline perthite and minor albite. It was collected in the eastern segment of the central intermediate unit (6), in the vicinity of layered saccharoidal albite.

Beryl T-24 was collected in the western part of the central intermediate unit (6), which consists of microcline perthite and quartz penetrated by the albite-rich assemblages of unit (3). It is white with a faint pink tint, short-prismatic (2×3 cm) and subhedral, and is associated with microcline perthite, quartz and minor oxide minerals of Ta. This specimen of primary beryl is one of the most alkali-rich so far analyzed from Tanco (Černý & Simpson 1977).

The crystals of emerald from New South Wales were found 9 km north-northeast of Emmaville, County Gough, approximately 500 km east-northeast of Sydney. They occur in weathered cassiterite-bearing veins in the Torington granite, associated with quartz, cassiterite, topaz, fluorite and arsenopyrite. They are pale green, cloudy, columnar crystals 50 mm in diameter and between 0.3 and 15 mm long. The crystals of emerald from Colombia are clear, dark green, and fragmented, ranging in size from 1×1 mm to 5×5 mm. They are from the Muzo mine, 105 km north of Bogota, in the province of Boyacá. The host rock is a thick sequence of Cretaceous shales and limestones. The

emerald occurs in calcite-albite veins associated with pyrite, quartz, fluorite, parisite and barite.

EXPERIMENTAL

Chemical analysis

Analyses for Li and Be were done on purified separates of alkali-bearing beryl by atomic absorption spectroscopy. Following the crystallographic work, the crystals used for the collection of intensity data were mounted in epoxy resin and polished.

TABLE 1. COMPOSITION AND UNIT FORMULAE OF ALKALI-BEARING BERYL

	SHEE-1-6	EEE-10	BLM503	T-24
SiO ₂	66.18	63.32	63.81	62.50
TiO ₂	0.00	0.02	0.01	0.01
Al ₂ O ₃	18.32	18.09	17.84	17.66
Fe ₂ O ₃	0.53	0.09	0.06	0.03
MnO	0.02	0.01	0.01	0.01
MgO	0.01	0.00	0.00	0.00
CaO	0.00	0.00	0.00	0.01
BeO	13.61	12.43	11.73	11.10
Li ₂ O	0.03	1.54	1.80	1.25
Na ₂ O	0.16	1.25	1.05	1.49
K ₂ O	0.01	0.02	0.03	0.03
Rb ₂ O	0.00	0.01	0.02	0.01
Cs ₂ O	0.06	1.98	2.76	3.56
Sum	98.93	98.76	99.12	97.66

	SHEE-1-6	EEE-10	BLM-503	T-24
Si	6.009	5.891	5.922	5.988
Al	1.961	1.984	1.977	1.995
Fe	0.036	0.006	0.004	0.002
Σ[6]	1.997	1.992	1.981	1.997
Be	2.963	2.787	2.690	2.555
Li	0.011	0.213	0.310	0.445
Σ[4]	2.974	3.000	3.000	3.000
K	0.001	0.002	0.004	0.004
Cs	0.002	0.078	0.111	0.145
Li	0.000	0.328	0.322	0.013
Na	0.028	0.225	0.191	0.277

TABLE 2. MISCELLANEOUS INFORMATION CONCERNING BERYL REFINEMENTS

	SHEE-1-6	EEE-10	BLM-503	T-24
a (Å)	9.206(1)	9.202(2)	9.210(2)	9.228(3)
c	9.185(2)	9.207(2)	9.230(2)	9.240(3)
V (Å ³)	673.8(2)	675.1(3)	678.0(4)	681.4(5)
Space group	P6/mcc	P6/mcc	P6/mcc	P6/mcc
Z	2	2	2	2
crystal size (mm)	0.24x0.28x0.36	0.22x0.24x0.28	0.22x0.34x0.40	0.25x0.35x0.38
Rad/Hono	Mo/Gr	Mo/Gr	Mo/Gr	Mo/Gr
R(av) %	1.0	1.4	0.7	1.1
Fo	817	812	815	825
Fo >σ	336	336	344	342
R(obs) %	2.7	2.4	2.6	3.2
wR(obs) %	3.1	2.7	3.2	3.4

$$R = \frac{\sum |F_o| - |F_c|}{\sum |F_o|}$$

$$wR = \left[\frac{\sum (|F_o| - |F_c|)^2 / \sum w F_o^2}{\sum w F_o^2} \right]^{1/2}, w = 1$$

TABLE 3. FINAL ATOMIC PARAMETERS FOR ALKALI-BEARING BERYL

	SHEE-1-6	EEE-10	BLM-503	T-24	
Si	x	0.3875(1)	0.3888(1)	0.3890(1)	0.3893(1)
	y	0.1158(1)	0.1181(1)	0.1185(1)	0.1192(1)
	z	0	0	0	0
	*U _{iso}	29(3)	51(3)	42(3)	70(3)
Be	x	1/2	1/2	1/2	1/2
	y	0	0	0	0
	z	1/4	1/4	1/4	1/4
	*U _{iso}	57(14)	94(13)	88(15)	122(17)
Al	x	2/3	2/3	2/3	2/3
	y	1/3	1/3	1/3	1/3
	z	1/4	1/4	1/4	1/4
	*U _{iso}	46(3)	54(3)	52(3)	54(4)
O(1)	x	0.3095(3)	0.3064(3)	0.3060(3)	0.3043(3)
	y	0.2362(3)	0.2354(3)	0.2354(3)	0.2349(3)
	z	0	0	0	0
	*U _{iso}	80(8)	119(8)	117(9)	147(10)
O(2)	x	0.4987(2)	0.4984(2)	0.4982(2)	0.4985(2)
	y	0.1454(2)	0.1468(2)	0.1469(2)	0.1477(2)
	z	0.1454(1)	0.1448(1)	0.1448(1)	0.1446(2)
	*U _{iso}	53(5)	102(5)	103(6)	145(7)
[Na]	x	0	0	0	0
	y	0	0	0	0
	z	0	0	0	0
	*U _{iso}	150**	129(42)	217(57)	251(42)
[Cs]	x	0	0	0	0
	y	0	0	0	0
	z	1/4	1/4	1/4	1/4
	*U _{iso}	150**	484(16)	367(16)	389(11)

* value given x10⁴

** value fixed during refinement

TABLE 4. SELECTED INTERATOMIC DISTANCES (Å) & ANGLES (°) IN BERYL

	SHEE-1-6	EEE-10	BLM-503	T-24
Si-O(1)	1.593(4)	1.599(3)	1.602(4)	1.610(4)
Si-O(1)a	1.595(2)	1.601(2)	1.603(2)	1.606(2)
Si-O(2)	x2 1.621(2)	1.612(1)	1.614(2)	1.614(2)
<Si-O>	1.608	1.606	1.608	1.611
O(1)-O(1)a	2.578(4)	2.556(3)	2.556(4)	2.549(4)
O(2)-O(1)a	x2 2.610(3)	2.608(2)	2.609(3)	2.617(4)
O(2)-O(1)	x2 2.639(4)	2.647(3)	2.650(3)	2.662(4)
O(2)-O(2)b	2.672(3)	2.667(2)	2.675(3)	2.671(4)
<O-O>Si	2.625	2.622	2.625	2.630
O(1)-Si-O(1)a	107.9(2)	106.0(2)	105.7(2)	104.9(2)
O(2)-Si-O(1)a	x2 108.5(1)	108.5(1)	108.4(1)	108.7(1)
O(2)-Si-O(1)	x2 110.4(1)	111.0(1)	111.0(1)	111.3(1)
O(2)-Si-O(2)b	111.0(1)	111.6(1)	111.9(1)	111.7(2)
<O-Si-O>	109.5	109.4	109.4	109.4
Be-O(2)	x4 1.652(2)	1.668(2)	1.672(2)	1.681(2)
O(2)-O(2)c	x2 2.688(4)	2.716(4)	2.722(4)	2.740(5)
O(2)-O(2)d	x2 2.355(3)	2.378(3)	2.385(3)	2.394(4)
O(2)-O(2)e	x2 3.010(4)	3.037(3)	3.043(4)	3.062(4)
<O-O>Be	2.684	2.710	2.717	2.732
O(2)-Be-O(2)c	x2 108.9(1)	109.0(1)	109.0(1)	109.2(1)
O(2)-Be-O(2)d	x2 90.9(1)	90.9(1)	91.0(1)	90.8(1)
O(2)-Be-O(2)e	x2 131.3(1)	131.1(1)	131.0(1)	131.1(1)
<O-Be-O>	110.4	110.3	110.3	110.4
Al-O(2)	x6 1.905(1)	1.904(1)	1.906(1)	1.906(2)
O(2)-O(2)g	x3 2.710(2)	2.703(2)	2.705(2)	2.703(3)
O(2)-O(2)d	x3 2.255(3)	2.378(3)	2.385(3)	2.394(4)
O(2)-O(2)f	x6 2.849(3)	2.839(2)	2.842(3)	2.837(3)
<O-O>Al	2.691	2.690	2.694	2.693
O(2)-Al-O(2)g	x3 90.7(1)	90.4(1)	90.4(1)	90.3(1)
O(2)-Al-O(2)d	x3 76.4(1)	77.3(1)	77.5(1)	77.8(1)
O(2)-Al-O(2)f	x6 96.8(1)	96.4(1)	96.4(1)	96.2(1)
<O-Al-O>	90.2	90.1	90.2	90.1
[Na]-O(1)	x6 2.578(2)	2.556(2)	2.556(2)	2.549(2)
[Na]-[Cs]	x2 2.296(1)	2.302(1)	2.307(1)	2.310(1)
[Cs]-O(1)	x12 3.452(2)	3.439(1)	3.443(2)	3.440(2)

Electron-microprobe analyses were done in the wavelength-dispersion mode on a Cameca Camebax SX50. The following standards were used: spodumene ($\text{SiK}\alpha$, $\text{AlK}\alpha$), almandine ($\text{FeK}\alpha$), $\text{NaScSi}_2\text{O}_6$ ($\text{NaK}\alpha$), Mn_2SiO_4 ($\text{MnK}\alpha$), diopside ($\text{CaK}\alpha$), olivine ($\text{MgK}\alpha$), titanite ($\text{TiK}\alpha$), orthoclase ($\text{KK}\alpha$), Rb microcline ($\text{RbK}\alpha$), pollucite ($\text{CsK}\alpha$). Data reduction was done using the 'PAP' Φ (ρz) routine of Pouchou & Pichoir (1985). The resulting compositions are given in Table 1.

TABLE 5. ^{29}Si MAS NMR PARAMETERS FOR BERYL

Sample	Half-width (Hz)	Chemical shift (ppm) Exp.	Calc.*
<u>Low-alkali beryl</u>			
SHEE-1-6	190	-102.3	-103.7
<u>Lithian-casian beryl</u>			
EEE-10	287	-101.9	
BIM-503	290	-101.3	
T-24 [2Be, 2Cs]	289	-100.9	-102.6
T-24 [Be, Li, 2Cs]			-102.5
T-24 [2Be, 1Cs]			-102.2
T-24 [2Be, 1Na]			-102.1
T-24 [2Be]			-101.8
<u>Emerald</u>			
Colombian	164	-102.5	-104.0
Australian	110	-102.4	

* Sherriff & Grundy (1991)
[] configuration of neighbouring cations used in calculation.

X-ray diffraction

Crystals used for the collection of the X-ray intensity data were selected on the basis of clarity, lack of optical zoning, lack of inclusions and equant shape. Cell dimensions were determined by least-squares refinement of the setting angles for 25 reflections aligned automatically on a four-circle diffractometer; values are given in Table 2. The intensity data were collected on a Nicolet R3m automated four-circle diffractometer according to the procedure of Hawthorne & Groat (1985). Reflections were measured over two asymmetric units out to $65^\circ 2\theta$ ($\sin \theta/\lambda = 0.758 \text{ \AA}^{-1}$); numbers of reflections are given in Table 2. Ten strong reflections uniformly distributed with regard to 2θ were measured at 10° intervals of ψ (the azimuthal angle corresponding to rotation of the crystal about its diffraction vector) from 0 to 350° . These data were used to calculate an ellipsoidal approximation to the shape of the crystal; this shape was then used to correct the normal data-set for absorption. The data were corrected for Lorentz, polarization and background effects, averaged and reduced to structure factors. A reflection was considered observed if its intensity I exceeds $4\sigma(I)$; total numbers of unique observed reflections for each crystal are given in Table 2, together with other information pertinent to data collection, reduction and refinement.

MAS NMR spectroscopy

The samples of alkali beryl and Australian emer-

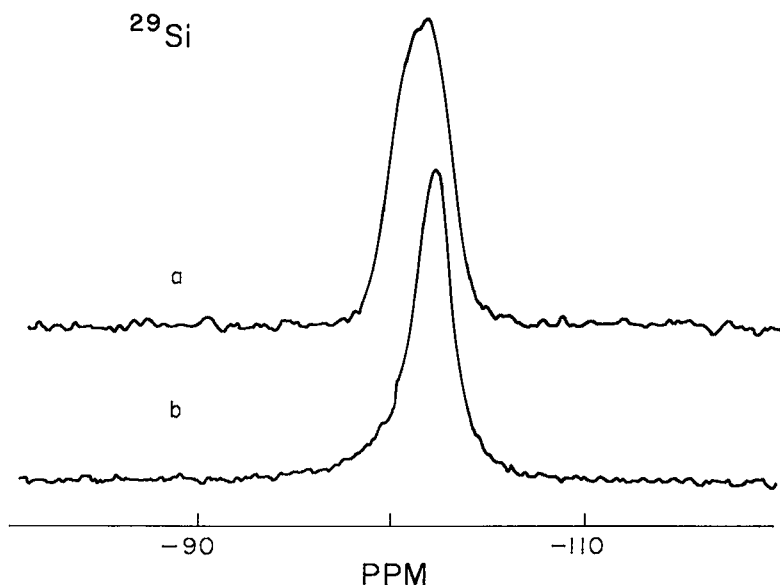


FIG. 1. ^{29}Si MAS NMR spectra: (a) T-24 Li-Cs beryl; (b) SHEE-1-6 low-alkali beryl.

ald were crushed to powders for packing into the NMR rotor; the gem-quality chips of emerald from Colombia were left intact (by request of the owner) and packed into the rotor as such. There was a relative enhancement of one of the peaks of the ^{27}Al quadrupolar spectrum of the Colombian emerald samples, but otherwise the resolution of the spectra from the chips is comparable to that from powdered samples.

A magic-angle spinning probe (Fyfe *et al.* 1982) with Delrin rotors was used with a Bruker WH-400 multi-nuclear Fourier Transform NMR spectrometer equipped with a 9.4 Tesla superconducting magnet to obtain the spectra from ^{29}Si , ^{27}Al , ^{23}Na , ^9Be and ^7Li . The samples were spun at approximately 3500 Hz at the magic angle of 54.7° to the magnetic field.

^{29}Si MAS NMR spectra were recorded at a frequency of 79.46 MHz with 8192 data points, a spectral width of 25000 Hz, 30° pulses and a 5-s delay between pulses. Chemical shifts were reproducible to ± 0.1 ppm (parts per million) and are reported in ppm of the magnetic field with reference to TMS (tetramethylsilane). ^{27}Al and ^{23}Na MAS NMR spectra were recorded at 104.23 and 105.80 MHz, respectively, with 15° pulses and a 0.3-s delay between pulses. The chemical shifts of ^{23}Na were measured with reference to a 0.1 M aqueous solution of NaCl, and those of ^{27}Al , to $[\text{Al}(\text{H}_2\text{O})_6]^{3+}$ in a saturated aqueous solution of $\text{Al}(\text{ClO}_4)_3$. MAS NMR spectra of ^7Li were measured at 155.5 MHz with reference to an aqueous solution of LiBr using a 5-s delay between pulses. ^9Be MAS NMR spectra were recorded at 56.2 MHz with a 0.1-s delay between pulses and with reference to an aqueous solution of $\text{Be}(\text{NO}_3)_2$. The delay between pulses for each nucleus was optimized to give the highest signal-to-noise level for the instrument time available.

^{133}Cs and ^6Li spectra were obtained on a Bruker MSL-300 multi-nuclear Fourier Transform spectrometer equipped with a high-speed Doty probe using 5-mm-diameter rotors. ^{133}Cs spectra were recorded at 39.37 MHz with a 5-s delay between pulses and are quoted with reference to 0.5 molal CsCl. ^6Li spectra were recorded at 44.17 MHz with a 10-s delay between pulses and are quoted relative to an aqueous solution of LiBr.

Structure refinement

Scattering curves for neutral atoms together with anomalous dispersion terms were taken from the International Tables for X-ray Crystallography (1974). *R* indices are of the form given in Table 2 and are expressed as percentages. Using the positional coordinates of Hawthorne & Černý (1977), together with site occupancies suggested by the chemical data, full-matrix least-squares refinement of all

variable parameters converged to the *R* indices given in Table 2. Final parameters are given in Table 3; tables of structure factors have been deposited with the Depository of Unpublished Data, CISTI, National Research Council of Canada, Ottawa, Ontario K1A 0S2. Selected interatomic distances and angles are given in Table 4.

RESULTS

^{29}Si

The chemical shift of the single peak in the ^{29}Si MAS NMR spectrum varies from -102.3 to -100.9 ppm with increasing alkali content (Table 5). The ^{29}Si MAS NMR peaks of EEE-10, BLM-503 and T-24, the Li-Cs-bearing samples, are 100 Hz wider than those of SHEE-1-6, the sample of low-alkali beryl (Fig. 1), and the samples of emerald (Table 5).

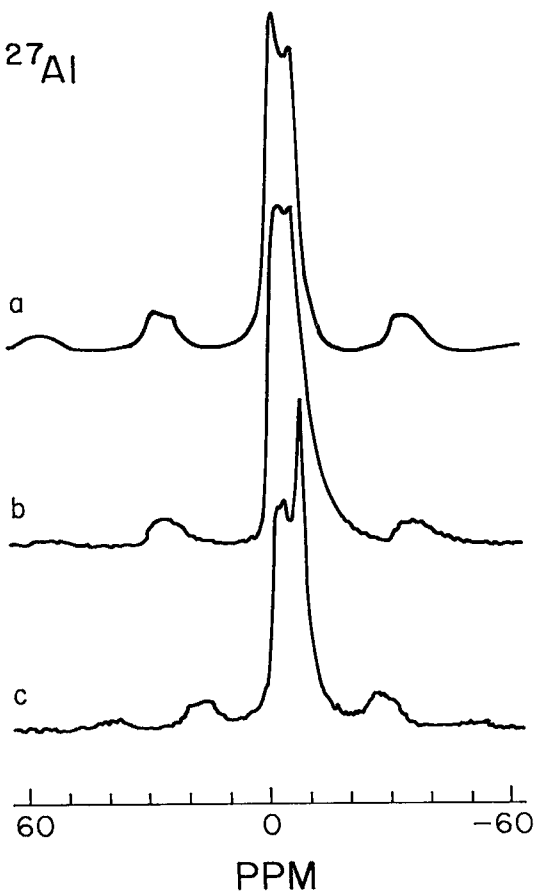


FIG. 2. ^{27}Al MAS NMR spectra: (a) SHEE-1-6 low-alkali beryl; (b) T-24 Li-Cs beryl; (c) chips of emerald from Colombia.

TABLE 6. ^{27}Al MAS NMR PARAMETERS FOR BERYL

Sample	Peak position (ppm)	Half-width (Hz)
Low-alkali beryl		
SHEE-1-6	-3.0, -7.5	840
Lithium-cesian beryl		
EEE-10	-3.2, -7.7	870
BLM-503	-3.7, -7.7	940
T-24	-4.0, -7.7	974
Emerald		
Colombian (chips)	-3.1, -4.4, -8.6	809
Australian	-2.9, -8.0	778

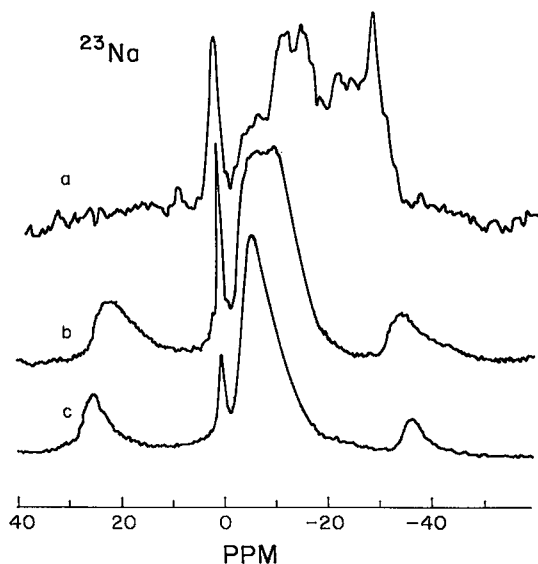


FIG. 3. ^{23}Na MAS NMR spectra: (a) SHEE-1-6 low-alkali beryl; (b) T-24 Li-Cs beryl; (c) T-24 Li-Cs beryl spinning at an angle of approximately 65° to the applied magnetic field. The narrow signal at 0 ppm is due to Na (as NaCl) in fluid inclusions.

In low-alkali beryl (including emerald), the local environment of Si will be ordered because of the lack of substituents at neighboring sites. For these minerals, the ^{29}Si signal is narrow. In beryl with a significant alkali content, there will be a range of local environments due to distortion of the structure to accommodate the alkali cations, interaction of Si with cations and H_2O occupying the channels, and variable occupancy of neighboring cation sites. This will produce a range of magnetic fields around the

Si atoms in the structure, and hence a range of chemical shifts in the MAS NMR spectrum. If the difference in chemical shift between different configurations is large relative to the intrinsic peak-width, then a series of discrete signals will result. If this shift is small relative to the peak width, then the signals strongly overlap and a single broadened signal results. By analogy with other spectroscopic methods, this can be designated as *substitutional broadening*, and is the case for the ^{29}Si MAS NMR spectra of alkali-rich beryl examined here.

^{27}Al

^{27}Al MAS NMR spectra of all samples of beryl have two maxima, at -3.2 and -7.7 ppm (Fig. 2, Table 6). The shape and half-width (peak width at half-height) of the peaks are consistent with the anisotropic environment and the large quadrupole moment of ^{27}Al . The half-width of the broad resonance increases with alkali content, from 840 Hz for SHEE-1-6 (low-alkali beryl) to 974 Hz for T-24 (Li-Cs beryl) (Table 6). This substitutional broadening is to be expected from the presence of local disorder associated with the $^{\text{IV}}\text{Li} \rightleftharpoons ^{\text{IV}}\text{Be}$ substitution in alkali-bearing beryl. In addition, the lack of any peak (around 60 ppm) that can be assigned to tetrahedrally coordinated Al is conformable with the $^{\text{IV}}\text{Li} \rightleftharpoons ^{\text{IV}}\text{Be}$ mechanism of substitution established by Bakakin *et al.* (1969) and Hawthorne & Černý (1977), and not with previously proposed models involving $^{\text{VI}}\text{Li} + ^{\text{IV}}\text{Al} + ^{\text{C}}\text{Na} \rightleftharpoons ^{\text{VI}}\text{Al} + ^{\text{IV}}\text{Be} + ^{\text{C}}\square$.

^{27}Al spectra of samples of emerald are similar to the others, except for a difference in the relative intensity of the two peaks, and an extra peak at -4.4 ppm in the spectrum of the Colombian emerald (Fig. 2c). ^{27}Al spectra of powdered samples of other samples of emerald have two peaks of approximately equal intensity, similar to the spectra of the other samples of beryl. As $^{\text{VI}}\text{Cr} \rightleftharpoons ^{\text{VI}}\text{Al}$ substitution does not change the immediate local environment of the remaining $^{\text{VI}}\text{Al}$, no difference is expected between the ^{27}Al MAS NMR spectra of low-alkali beryl and emerald. The extra peaks in the spectra of the emerald samples from Colombia are attributed to inclusions of shale, which give ^{27}Al peaks in the same region as the signal from $^{\text{VI}}\text{Al}$ in the emerald.

^{23}Na

Na has a broad quadrupolar doublet at about 10 ppm in the ^{23}Na MAS NMR spectrum (Fig. 3b). The spectrum of SHEE-1-6, which has the lowest concentration of Na, has, in addition, poorly resolved peaks between -5 and -35 ppm (Fig. 3a); these could be due to Na in defects, or along grain boundaries. Such peaks would not be obvious in the spectra of more sodic samples, as they would be hid-

den by the strong peak due to Na in the channels. Quadrupolar effects can be reduced by spinning the sample at angles to the magnetic field other than the magic angle (Ganapathy *et al.* 1982). As the angle between the rotational axis of the sample and the applied magnetic field H_0 is increased, the quadrupolar doublet from ^{23}Na at the channel site collapses to a singlet and becomes narrower (Fig. 3c). Most of the ^{23}Na spectra also have a narrow peak at 0 ppm (Fig. 3) due to NaCl in solution in the fluid inclusions (Sherriff *et al.* 1987).

^9Be

^9Be MAS NMR spectra of low-alkali beryl and the Colombian emerald all have one broad symmetrical peak at about -2.4 ppm (Table 7, Fig. 4a). In the spectra of Li-Cs-bearing beryl, the peak is narrower and asymmetrical, with a maximum at -1.6 and a shoulder at -2.6 ppm (Table 7, Fig. 4b). The situation here is not clear at all. Possibly there are two local environments for Be in Li-Cs-bearing beryl, one similar to that in low-alkali beryl and emerald, and the other producing an additional narrower peak at -1.6 ppm. As an alternative, the peak asymmetry may be due to quadrupolar effects (that consequently must differ from those in low-alkali beryl). Whichever possibility is the case, the signal half-width decreases significantly with increasing alkali content. This is not observed for any other of the nuclei examined. No explanation is immediately apparent.

TABLE 7. ^9Be MAS NMR PARAMETERS FOR BERYL

Sample	Peak position (ppm)	Half-width (Hz)
Be(NO ₃) ₂ (saturated aqueous solution)	0	130
SHEE-1-6	Low-alkali beryl	
	-2.5	215
EEE-10 BLM-503 T-24	Lithian-cesian beryl	
	-1.6 -2.6	132
	-1.6 -2.6	136
	-1.6 -2.6	119
Colombian	Emerald	
	-2.3	244

^6Li and ^7Li

The beryl samples with a high Li content give two ^7Li MAS NMR peaks: a strong narrow peak at 0.8 ppm and a small peak at -1.6 ppm (Table 8, Fig. 5). Sample BLM-503, which has the highest Li content, gives the largest peak at -1.6 ppm in the ^7Li spectrum, and is the only sample to show this peak in the less-well-resolved ^6Li spectrum. The relative intensities of the two peaks are 15:1 for EEE-10, 12:1 for BLM503, and 21:1 for T-24. The 2.4 ppm difference between the two MAS NMR peaks suggests different environments. These could be channel sites, tetrahedrally coordinated sites, or Li in solution in

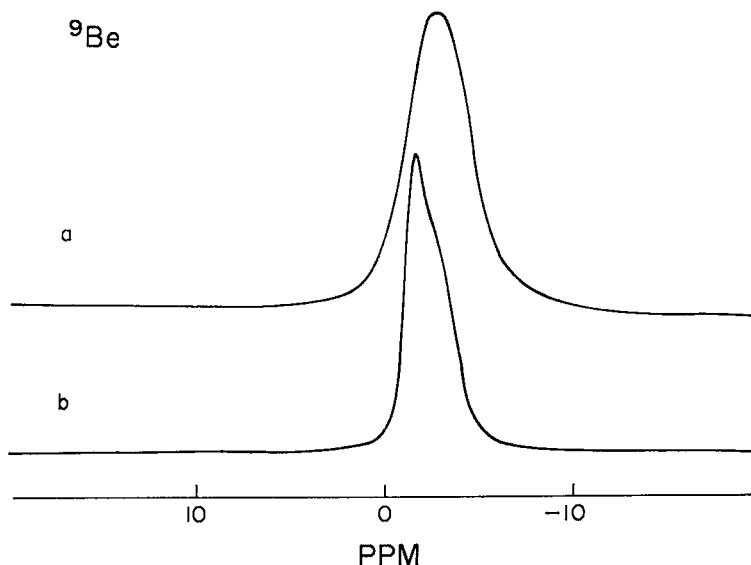


FIG. 4. ^9Be MAS NMR spectra: (a) SHEE-1-6 low-alkali beryl; (b) T-24 Li-Cs beryl.

TABLE 8. ^7Li AND ^6Li MAS NMR PARAMETERS FOR BERYL

Sample	Peak position (ppm)	Half-width (Hz)
^7Li (155.5 MHz)		
LiBr (saturated aqueous solution)	0	140
SHEE-1-6	Low alkali beryl 0.5	488
EEE-10	Lithian-cesian beryl 0.7 -1.6	146
BLM-503	0.6 -1.6	156
T-24	0.6 -1.6	156
^6Li (44.2 MHz)		
LiBr (saturated aqueous solution)	0	17
SHEE-1-6	Low alkali beryl no signal	
EEE-10	Lithian-cesian beryl 0.8	51
BLM-503	0.8 -1.6	43
T-24	0.8	46

the fluid inclusions. The latter possibility is ruled out, as no signal was observed in a static ^7Li spectrum. Presumably, one ^7Li peak is due to Li at channel sites, and the other to Li replacing Be in tetrahedral coordination. Tetrahedrally coordinated Li would be more shielded than Li in the channel; therefore, the

strong peak at 0.8 ppm is assigned to Li in the channel, and the weak peak at -1.6 ppm is assigned to Li replacing Be in tetrahedral coordination. The relative intensities of the two peaks are not proportional to the amount of Li estimated (from the chemical analyses) to be at each site; this could be due to different rates of spin-lattice relaxation. Li at the channel site could have more rotational freedom of movement, and hence, a more efficient mechanism of dipolar relaxation than Li at the tetrahedral site; this would enhance the ^6Li and ^7Li peaks from the channel site.

The low-alkali sample, SHEE-1-6, gave no ^6Li signal and a weak ^7Li spectrum, with a broad peak and large spinning sidebands (Fig. 5a). This signal may be due to small amounts of Li in a variety of environments, possibly along grain boundaries or associated with structural defects, as well as in fluid inclusions. As with ^{23}Na , these minor peaks vanish into the baseline when a strong peak is recorded in the spectrum.

^{133}Cs

The ^{133}Cs spectra all have a broad peak (half-width of 950 Hz) at -18 ± 1 ppm, with strong spinning sidebands; cubic CsCl gives a narrow peak at 223.2 ppm with negligible spinning sidebands. The broad peak and high spinning-sideband intensity in the beryl spectra are consistent with the anisotropic environment of Cs in the channels of beryl.

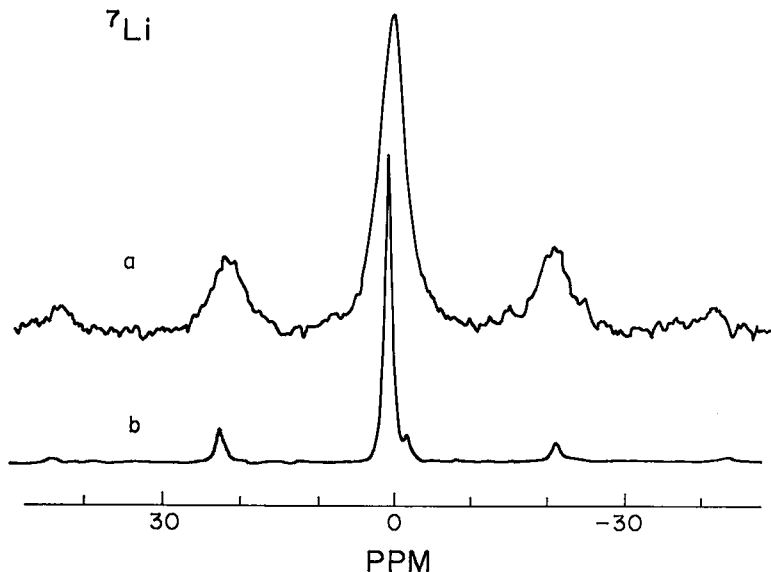


FIG. 5. ^7Li MAS NMR spectra: (a) SHEE-1-6 low-alkali beryl; (b) T-24 Li-Cs beryl.

SHORT-RANGE ORDER IN BERYL

²⁹Si

Each SiO₄ tetrahedron links to two other ring tetrahedra, two BeO₄ tetrahedra and two AlO₆ octahedra. In the beryl samples examined here, no significant substitutions occur in the Al octahedra or the neighboring SiO₄ tetrahedra; thus the variation in next-nearest neighbors involves primarily the BeO₄ tetrahedra, which may be occupied either by Be or Li. Further variation occurs as a result of alkali = vacancy substitution in the channel. In terms of tetrahedrally coordinated next-nearest neighbors, we may identify three different configurations: [2Si,2Be], [2Si,Be,Li] and [2Si,2Li]. In general, the Li occupancy of the Be site is less than 0.20; if the local configurations are totally disordered, then the number of [2Si,2Li] configurations will be low, and the spectra will be dominated by the [2Si,2Be] and [2Si,Be,Li] configurations. Although a large number of potential channel configurations exist, the major effect will depend only on whether or not an adjacent channel site is occupied (and not which alkali occupies that site). The presence or absence of a neighboring alkali cation would double the number of potential configurations to four, and the variable chemical identity of the alkalis would produce additional substitutional broadening.

We can test this explanation of our broadened signals for ²⁹Si in Cs–Li-bearing beryl using the method of calculating ²⁹Si chemical shifts developed by Sherriff & Grundy (1988, 1991). Starting from the observed structure, a geometrical model was developed for each local configuration using graphical modeling; the resulting arrangements are used in the calculation of the chemical shift (Table 5).

Three factors affect the calculated chemical shifts for low-alkali and Li–Cs-bearing samples of beryl: (i) the Si–O and Al–O distances for Li–Cs-bearing beryl are greater than for low-alkali beryl (Table 4). This results in a calculated shift of about 2 ppm to low field, explaining the shift to low field with increasing alkali content; (ii) the replacement of Be by Li causes a shift of only 0.1 ppm to low field, and (iii) Cs or Na in the channels causes a shift to high field of 0.4 ppm per adjacent Cs or Na.

The broadness of the peaks in Li–Cs-bearing beryl (290 Hz) (compared with those of low-alkali beryl) (190 Hz) is caused by overlapping peaks from Si[2Si,Al] with [Be,Li], [2Be] or [2Li] next-nearest-neighbor configurations with either [Na], [Cs] or [2Cs] in the channels. These peaks are between 2 and 3 ppm wide, and individual peaks less than 1 ppm apart will not be resolved. We may calculate the width of the substitutionally broadened peaks from the peak width of the low-alkali beryl (SHEE-1-6) and the spread of the calculated shifts of the local

configurations in alkali beryl (T-24); the resulting value is 190 + 80 = 270 Hz, in good agreement with the observed value of 290 Hz.

The chemical shift calculated for anhydrous emerald is –104.0 ppm, 0.3 ppm to higher field than the values for the low-alkali beryl structures, in agreement with the 0.2 ppm difference between the measured values.

²⁷Al

Substitutional broadening in the ²⁷Al spectra of Cs–Li-bearing beryl indicates different local configurations. The local symmetry allows four possible local arrangements around an AlO₆ octahedron: [3Be], [2Be,Li], [Be,2Li] and [3Li]. As Be is always much more important than Li, the latter two have low probability (unless there is strong local order, for which there is no evidence), and only the first two arrangements will occur in significant amounts.

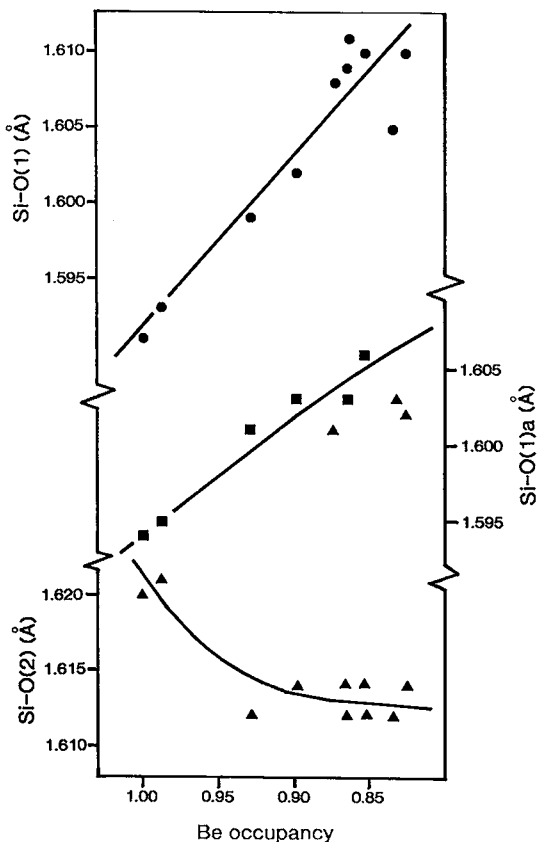


FIG. 6. Variation in Si–O bond lengths with decreasing Be content of the Be site in alkali-bearing beryl. Samples from this study, Hawthorne & Cerný (1977), Brown & Mills (1986), Aurisicchio *et al.* (1988).

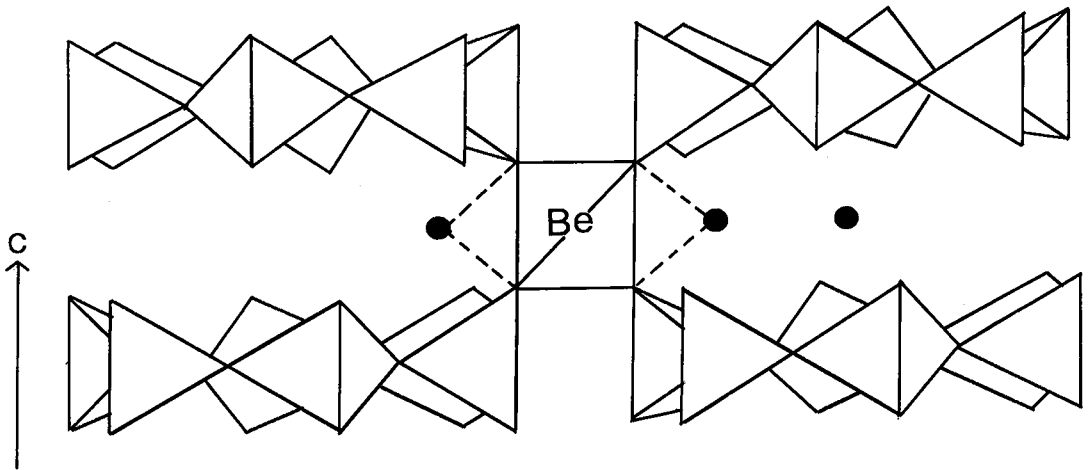


FIG. 7. Schematic illustration of the beryl structure: (•) indicates possible positions for Li.

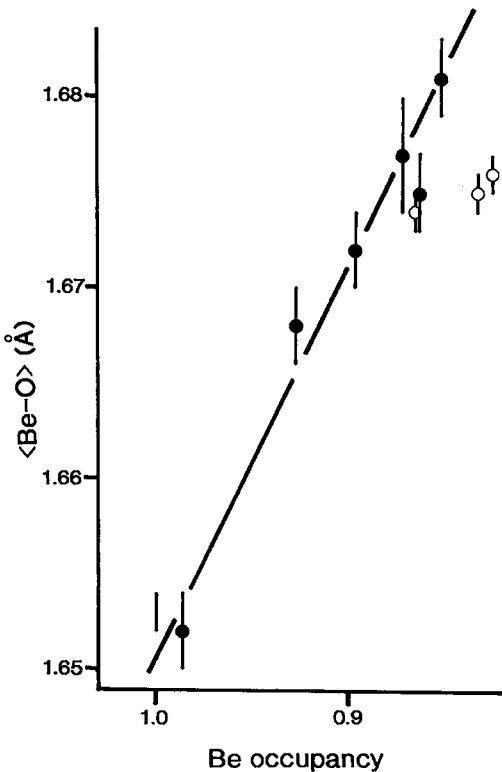
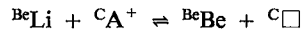


FIG. 8. Variation in <Be-O> as a function of Be content of the Be site in alkali-bearing beryl. Full circles: this study, Hawthorne & Černý (1977), Brown & Mills (1986); open circles: Aurisicchio *et al.* (1988); vertical dash: mean value for samples of synthetic alkali-free beryl.

LONG-RANGE ORDER IN BERYL

The Li ⇌ Be substitution

Bakakin *et al.* (1969), Hawthorne & Černý (1977) and Aurisicchio *et al.* (1988) proposed that Li directly replaces Be at the Be-site. This may be written as



where A⁺ denotes alkali metals, and the superscripts denote the sites at which the substitutions take place (Be: Be site, C: channel site). Manier-Glavinaz *et al.* (1989a, b) have questioned the validity of this mechanism on the basis of hydrothermal leaching and exchange studies; they concluded that "none of our results supports the substitution of Li for Be". A closer look at this mechanism is thus required.

The role of Li: the first important point to make is that Li is *essential* to the substitution involving a decrease in the Be content of beryl; thus it is always observed that Li is greater than or equal to (3-Be). If Li behaved as a normal channel cation (*i.e.*, like Na or Cs), this particular relationship need not occur, the charge deficiency caused by the decrease in Be could be compensated solely by the presence of Na and Cs. The fact that Li is always present [and in excess of (3-Be)] shows that Li must be playing a different role to that of Na and Cs in alkali-bearing beryl.

Local bond-valence arguments: In alkali-free beryl, the bond-valence sum at O(2) is 2.00 v.u. Loss of the Be reduces the sum to 1.5 v.u.; how is this discrepancy compensated? To some extent, this can be done as proposed by Hawthorne & Černý (1977):

the structure adjusts by shortening the Si-O(2) bond and lengthening both Si-O(1) and Si-O(1a) bonds, the resultant deficiency at O(1) being compensated by bonding from the channel alkali atoms that are part of the ${}^{\text{Be}}\text{Li} + {}^{\text{C}}(\text{Na}, \text{Cs}) \rightleftharpoons {}^{\text{Be}}\text{Be} + {}^{\text{C}}\square$ mechanism of substitution. Figure 6 shows this to be the case for continuous substitution; Si-O(1) and Si-O(1a) gradually lengthen with decreasing Be and Si-O(2) decreases. It is interesting that the Si-O(2) bond seems to have a limiting value of $\sim 1.612 \text{ \AA}$; possibly the extent of Li substitution in sample T-24 is the limit of Li incorporation at the Be site in beryl.

Although this mechanism looks reasonable, it is not sufficient to compensate for the loss of the Be; O(2) needs to bond directly to an additional atom. The only possibility (in natural beryl) is Li, in line with our previous argument that Li must be an integral part of the substitution mechanism at the local scale. Two arrangements allow Li to bond to O(2): (i) Li may occupy the central Be position, and bond to all four O(2) oxygen atoms; (ii) Li may occupy a position in the channel but close to the (BeO_4) tetrahedron, such that it bonds to two of the four O(2) oxygen atoms (Fig. 7). For possibility (ii), Li must have long bonds to other anions (and possibly H_2O) to satisfy its own bond-valence requirements; thus from a local bond-valence viewpoint, both of these models are possible.

Charge-balance requirements: the two models suggested above have quite different implications concerning charge balance. For model (i), Li^+ replaces Be^{2+} , and further alkali substitution in the channel is required for overall charge-balance. For model (ii), 2Li^+ replace Be^{2+} and *this is a charge-balanced substitution*; thus model (ii) cannot account for the presence of Na + Cs in the channels.

Mean bond-length variations: the effect of the Li for Be substitution on the mean bond-length of the (BeO_4) tetrahedron is examined in Figure 8. There is a well-developed linear relationship between size of tetrahedron and Be content. The variation in $\langle \text{BeO} \rangle$ observed in Figure 8 is expected if Li replaces Be at the Be-site; thus Figure 8 agrees with quantitative predictions of model (i). Such a variation also is possible with model (ii), if the size of a vacancy at the Be-site is the same as the size of ${}^{\text{IV}}\text{Li}$. However, in our opinion, Figure 8 supports model (i) more strongly than model (ii).

Infrared-absorption spectroscopy: if Li replaces Be in sufficient amounts at the Be-site, the vibrational region of the infrared-absorption spectrum should show absorptions corresponding to LiO_4 vibrations. As shown by Tarte (1964), LiO_4 vibrations occur in the $400\text{--}600 \text{ cm}^{-1}$ region. Manier-Glavinaz *et al.* (1989b) did not observe any peaks that they assigned to LiO_4 in this region. On the other hand, Aurisicchio *et al.* (1990) observed "weak shoulders" at 700 cm^{-1} and 560 cm^{-1} in low-

temperature spectra of Li-bearing beryl, noted that the intensities of these shoulders correlate with the amount of Li, and assigned these bands to LiO_4 vibrations.

Assessment of the models: we believe that the arguments still support direct replacement of Be by Li at the Be-site. The strongest point is that involving the combination of local bond-valence and (long-range) charge-balance requirements. Substitution of Li outside the (BeO_4) tetrahedron requires 2Li per Be to satisfy local bond-valence requirements; however, this also satisfies long-range charge-balance requirements and cannot account for the presence of Na and Cs in the channels. Furthermore, many samples of beryl do not have sufficient Li to satisfy this mechanism. Thus we conclude that Li does replace Be at the Be-site.

Channel site-occupancies

This is a non-trivial problem, as we are trying to assign up to six scattering species (Na, K, Rb, Cs, Li, H_2O) to two (or more) sites in the channel. In any one particular case, no solution to this problem is unique, and the most we can hope for is a model that is consistent with all the crystal-chemical considerations. In view of these difficulties, it is not surprising that two contrasting models are currently extant. Hawthorne & Černý (1977) assigned Na to the 2b site at (0,0,0) and (K + Rb + Cs + H_2O) to the 2a site at (0,0, $\frac{1}{4}$); this scheme also was used by Brown & Mills (1986). Aurisicchio *et al.* (1988) assigned (H_2O) to the 2b site and (Na, K, Rb, Cs) to the 2a site, and applied the scheme to fifteen structure refinements of beryl; however, they do make the comment that the site assignments of Na and H_2O used by Hawthorne & Černý (1977) and Brown

TABLE 9. ELECTRON DENSITIES ASSOCIATED WITH THE 2a AND 2b CHANNEL SITES, AND THE CHANNEL SCATTERING SPECIES FOR ALKALI-BEARING BERYL

	SHEE-1-6	EEE-10	HB-3*	BLM-503	T-24	1*
2a	1.19	9.11	10.30	11.42	13.86	15.5
2b	0.46	2.15	3.21	2.32	3.43	3.4
Total	1.65	11.26	13.51	13.74	17.29	18.9
Cs	0.11	4.29	4.95	6.11	7.98	7.37
Na	0.31	2.48	2.31	2.10	3.05	3.44
Rb	0.00	0.04	-	0.04	0.04	0.24
K	0.02	0.04	0.95	0.08	0.08	0.62
Li	-	0.98	-	0.97	0.04	0.15
Total Alkalies	0.44	7.83	8.21	9.30	11.19	11.82
H_2O^{**}	1.21	(3.43)	4.40	4.44	(6.10)	6.60
Total (all)	(1.65)	(11.26)	12.61	(13.74)	(17.29)	18.42

* Data from Hawthorne & Černý (1977)

+ Data from Brown & Mills (1986)

** values in parentheses were calculated as indicated in the text.

& Mills (1986) also may be correct. As the resolution of this question is of considerable interest, we will examine it in some detail.

Cs in the channel

In the refinements of high-Cs beryl (Hawthorne & Černý 1977, Brown & Mills 1986, Aurisicchio *et al.* 1988, samples 19, 20 and 22; this work, samples EEE-10 and T-24), the scattering power of Cs dominates the net scattering from the channel species. As the majority of the electron density resides at the 2a position (Table 9), most of the Cs *must* occur at this site. Even if we assign small amounts of Cs to the 2b position, the remaining (Cs + other alkalis + H₂O, where known) exceeds full occupancy of that site, a physical impossibility. Consequently we conclude from this combination of diffraction and chemical data that Cs is highly ordered at the 2a site.

H₂O in the channel

Aurisicchio *et al.* (1988) refined the structures of two samples of (red) anhydrous beryl with small amounts of alkalis in the channel. They found that the only electron density in the channel was located at the 2a position, and thus all of the alkalis (including Na) in the channel of these two crystals must be at the 2a site. They used this as the basis for the general scheme that all alkalis occur at 2a and all (H₂O) occurs at 2b. On the other hand, Gibbs *et al.*

(1968) and Morosin (1972) refined structures of synthetic hydrous alkali-free beryl; both studies observed electron density at the 2a site, which they (unavoidably) assigned to H₂O. These two results are not incompatible, but the second result does show that one cannot conclude from the first result that H₂O always occurs at the 2b site.

In Table 9, we summarize the electron densities at the 2a and 2b positions for the refinements in which we have that information, together with the electron density associated with each chemical species of alkali in the channel. For these, we refined the 2a and 2b site-occupancies unconstrained by chemistry; where the concentration of H₂O was determined, there is reasonable agreement between the total electron density in the channel given by the refinement and that calculated from the chemical analysis. For other crystals, we calculated the H₂O by subtracting the electron density due to the alkalis from the total electron density in the channel.

The electron densities observed at the 2b position in all of the samples of beryl in Table 9 are less than the electron densities attributable to channel H₂O. Consequently H₂O *cannot* solely occupy the 2b position; considerable amounts of H₂O (nearly all of the H₂O in sample SHEE-1-6) must occupy the 2a site. This contrasts with the findings of Aurisicchio *et al.* (1988); the reasons for this difference are not clear.

OH in the channel

Both Manier-Glavinaz *et al.* (1989b) and Aurisicchio *et al.* (1990) have assigned specific bands in the infrared-absorption spectra of both natural and leached samples of beryl to principal (OH) stretches. On the basis of its temperature behavior and intensity behavior as a function of composition, Aurisicchio *et al.* (1990) assigned a band at 3663 cm⁻¹ to (OH) associated with Na (and also to type-II H₂O). On the other hand, Manier-Glavinaz *et al.* (1989b) assigned a band at ~ 3700 cm⁻¹ to (OH). This specific band is present as a weak shoulder in their sample of natural beryl, and increases in intensity with loss of alkalis on leaching; thus its assignment to (OH) cannot be questioned. From a (long-range) charge-balance viewpoint, one can argue that this H must bond to a framework oxygen [rather than exist as an (OH)⁻ channel species]. It seems reasonable that such H will attach itself to O(2), occupying a position somewhat similar to Li in Figure 7.

The situation with regard to the (OH) bond assigned at 3663 cm⁻¹ is less clear. Although Aurisicchio *et al.* (1990) suggested that this is the case, it is not clear how the bond-valence requirements of the associated oxygen will be satisfied. The maximum coordination attained by such an oxygen is [2Na + H]. Assuming negligible hydrogen-

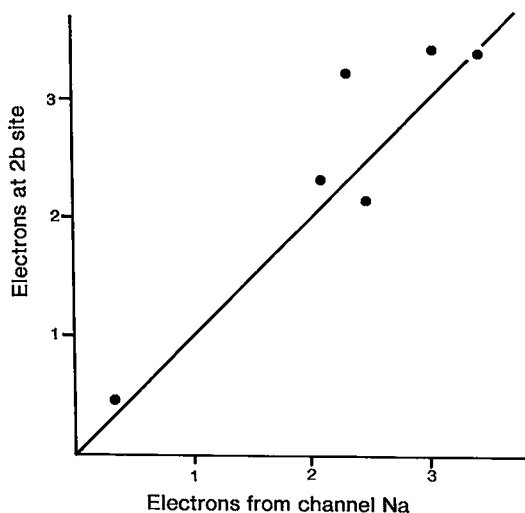


FIG. 9. The observed electron density at the 2b position in alkali-bearing beryl *versus* the electrons due to Na in the structure; the line is not a least-squares line, but represents the 1:1 relationship.

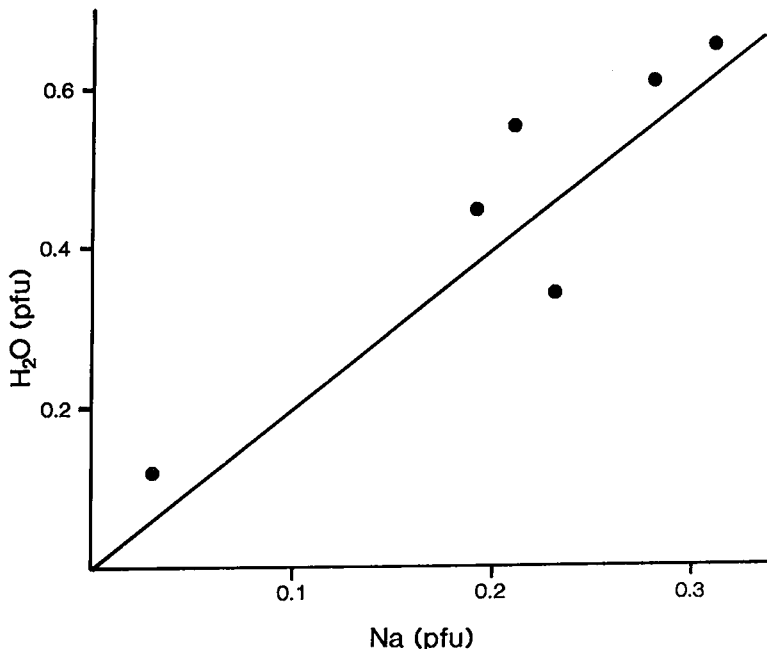


FIG. 10. H₂O versus Na in alkali-bearing beryl; the line represents a 2:1 relationship between the two variables.

bonding, each Na–O bond must have a bond valence of 0.5 v.u. for the oxygen of the (OH)-group to be satisfied. Use of the equation of Brown (1987) indicates an Na–OH bond length of 1.2 Å, shorter than any Na–O distances observed in inorganic solids. Thus although the argument put forward by Aurisichio *et al.* (1990) to justify their assignment (*i.e.*, the strong temperature-dependence of the band intensity) seems reasonable, there are some unanswered questions about the local stereochemistry resulting from this assignment.

Na in the channel

Two possibilities for the occurrence of Na in the channels have been proposed. Based on crystal-chemical arguments, Hawthorne & Černý (1977) assigned Na to the 2b site, and this scheme also was used by Brown & Mills (1986). Conversely, Aurisichio *et al.* (1988) assigned Na to the 2a site, based on the results for anhydrous (red) beryl, which has no H₂O and no electron density at the 2b site. Figure 9 shows a comparison of the electron density at the 2b position and the electrons due to channel Na in examples of alkali-bearing beryl for which this information is available. The 1:1 correlation may suggest that the electron density at the 2b position is due to Na occupancy of that site.

Hawthorne & Černý (1977) proposed that Na is

bonded to 2 H₂O groups at adjacent sites in the channel. This scheme is examined for alkali-bearing beryl in Figure 10. The data scatter about the line $\text{Na} = \frac{1}{2}\text{H}_2\text{O}$, suggesting that this is the case. This model does produce a slight bond-valence excess at the Na atom, but this could easily be removed by slight positional displacement of the H₂O group off the 2b site.

Li in the channel

The size of the cavity around the 2a position is far too large for the bond-valence requirements of a central Li cation to be satisfied, even with H₂O groups at adjacent 2b sites. If Li occurs at the 2b position, the bond-valence sum is ~ 0.75 v.u. if we assume that Li bonds to 2H₂O groups at adjacent 2a sites; this sum is still too low. There are two possibilities here: either Li occupies the 2b position and adjacent H₂O groups are strongly displaced off the adjacent 2a sites toward the Li, or the Li occurs at disordered positions within the channel.

Let us consider the first possibility. We have already assigned essentially all H₂O to be bonded to Na. However, the Na was found to have an excess of bond valence in this configuration [Na–(H₂O)²]. This could be alleviated by displacement of one or both of the H₂O groups at the 2a position away from the Na. If the adjacent 2b site(s) is occupied

by Li, this will increase the bond valence at Li to the ideal value of 1 v.u. Hence one can propose a reasonable model in crystal-chemical terms for the occupancy of the 2b position by Li.

Let us consider the second model. If Li is disordered about the channel, it approaches more closely the anions in the wall of the channel, thus increasing its bond-valence sum. At these disordered positions, it could also bond to an H₂O group. It is possible that the coordination number in the disordered position is lower, although it may vary with the exact details of the local positions.

CONCLUSIONS

The current situation with regard to cation order in alkali-bearing beryl may be summarized as follows:

Short-range order

1. The ²⁹Si signal is narrow in low-alkali beryl, and broadens with increasing alkali content. This is the result of different local next-nearest-neighbor configurations produced by the incorporation of alkalis into the beryl structure, and is here called *substitutional broadening*, after analogous effects in other forms of spectroscopy. The amount of substitutional broadening may be calculated from the correlation of Sherriff & Grundy (1991) using simulated local stereochemistries.

2. The ²⁷Al spectra show only [VI]-coordinate Al to be present in alkali-bearing beryl, and these spectra also show substitutional broadening.

3. Two ⁷Li and ⁶Li signals are observed, indicating that Li occurs both as a framework substituent and as a channel constituent.

4. With continuing alkali enrichment, Na equals ½(H₂O), suggesting that Na is coordinated by two H₂O groups in the channel (Hawthorne & Černý 1977, this study).

Long-range order

1. The <Be-O> distance expands linearly with increasing Li ⇌ Be substitution, but the O-Be-O bond angles remain unchanged (Hawthorne & Černý 1977, Brown & Mills 1986, Aurisicchio *et al.* 1988).

2. The bond-valence deficiency produced at O(2) by the Li ⇌ Be substitution is compensated by a lengthening of Si-O(1) and Si-O(1)a and a shortening of Si-O(2) (Hawthorne & Černý 1977, Aurisicchio *et al.* 1988).

3. Alkali-bearing beryl shows residual electron-density in the channels, with that at the 2a position always exceeding that at the 2b position.

4. Cs occurs at the 2a position (Bakakin *et al.*

1969, Hawthorne & Černý 1977, Brown & Mills 1986, Aurisicchio *et al.* 1988).

5. The electron densities observed at the 2b positions across the alkali-bearing beryl series are compatible with all Na ordered at 2b; they are not compatible with all H₂O ordered at 2b, but do not preclude 2b occupied by H₂O with Na and additional H₂O at 2a. The former model is simpler, but a neutron-diffraction refinement of the structure of a sample of alkali- and H₂O-rich beryl is required to unequivocally distinguish between these two possibilities.

ACKNOWLEDGEMENTS

We are grateful to T. Ottaway, Royal Ontario Museum, for the samples of emerald (which she made us give back). Dr. R.E. Lenkinski and Mr. W. Klimstra of the South-western Ontario NMR centre are thanked for assistance with NMR instrumentation, Professor C.A. Fyfe, University of British Columbia, for the design of the MAS probe, Dr. J.A. Ripmeester of the National Research Council of Ottawa for use of his MSL spectrometer and for helpful discussions, W. Blonski and R. Chapman for help with atomic absorption and electron-microprobe analyses, respectively. This work was funded by the Natural Sciences and Engineering Research Council of Canada through a postgraduate scholarship to BLS, operating grants to HDG, JSH, FCH and PC, major equipment and infrastructure grants to FCH, and a major installation grant to PC. We thank the referees for helpful reviews of the paper.

REFERENCES

- AURISICCHIO, C., FIORAVANTI, G., GRUBESSI, O. & ZANAZZI, P.F. (1988): Reappraisal of the crystal chemistry of beryl. *Am. Mineral.* **73**, 826-837.
- , GRUBESSI, O. & ZECCHINI, P. (1990): Reappraisal of infrared spectroscopy of beryl. *Int. Mineral. Assoc., 15th Gen. Meet., Abstr.*, 421.
- BAKAKIN, V.V., RYLOV, G.M. & BELOV, N.V. (1969): Crystal structure of a lithium-bearing beryl. *Dokl. Acad. Sci. U.S.S.R.* **188**, 659-662.
- BEUS, A.A. (1960): *Geochemistry of Beryllium and Genetic Types of Beryllium Deposits*. Publ. House Acad. Sci., Moscow.
- BROWN, G.E., JR. & MILLS, B.A. (1986): High-temperature structure and crystal chemistry of hydrous alkali-rich beryl from the Harding pegmatite, Taos County, New Mexico. *Am. Mineral.* **71**, 547-556.
- BROWN, I.D. (1987): Recent developments in the bond valence model of inorganic bonding. *Phys. Chem. Miner.* **15**, 30-34.

- BRAGG, W.L. & WEST, J. (1926): The structure of beryl $\text{Be}_3\text{Al}_2\text{Si}_6\text{O}_{18}$. *Proc. R. Soc. London, Ser. A III*, 691-714.
- ČERNÝ, P. (1975): Alkali variations in pegmatitic beryl and their petrogenetic implications. *Neues Jahrb. Mineral. Abh.* **123**, 198-212.
- _____ (1982): The Tanco pegmatite at Bernic Lake, southeastern Manitoba. In *Granitic Pegmatites in Science and Industry* (P. Černý, ed.). *Mineral. Assoc. Can., Short Course Handbook* **8**, 527-543.
- _____ (1989): Exploration strategy and methods for pegmatite deposits of tantalum. In *Lanthanides, Tantalum, and Niobium* (P. Moller, P. Černý & F. Saupe, eds.). Springer-Verlag, New York (274-302).
- _____, FRYER, B.J., LONGSTAFFE, F.J. & TAMMEMAGI, H.Y. (1987): The Archean Lac du Bonnet batholith, Manitoba: igneous history, metamorphic effects and fluid overprinting. *Geochim. Cosmochim. Acta* **51**, 421-438.
- _____ & SIMPSON, F.M. (1977): The Tanco pegmatite at Bernic Lake, Manitoba. IX. Beryl. *Can. Mineral.* **15**, 489-499.
- _____, TRUEMAN, D.L., ZIEHLKE, D.V., GOAD, B.E. & PAUL, B.J. (1981): The Cat Lake, Winnipeg River and the Wekusko Lake Pegmatite Fields, Manitoba. *Man. Dept. Energy and Mines, Mineral Res. Div. Geol. Rep.* ER80-1.
- FYFE, C.A., GOBBI, G.C., HARTMAN, J.S., LENKINSKI, R.E., O'BRIEN, J.H., BEANGE, E.R. & SMITH, M.A.R. (1982): High-resolution solid-state MAS spectra of ^{29}Si , ^{27}Al , ^{11}B and other nuclei in inorganic systems using a narrow-bore 400-MHz high-resolution nmr spectrometer. *J. Magn. Res.* **47**, 168-173.
- GANAPATHY, S., SCHRAMM, S. & OLDFIELD, E. (1982): Variable-angle sample-spinning high resolution NMR of solids. *J. Chem. Phys.* **77**, 4360-4365.
- GIBBS, G.V., BRECK, D.W. & MEAGHER, E.P. (1968): Structural refinement of hydrous and anhydrous synthetic beryl, $\text{Al}_2(\text{Be}_3\text{Si}_6)\text{O}_{18}$ and emerald, $\text{Al}_{1.9}\text{Cr}_{0.1}(\text{Be}_3\text{Si}_6)\text{O}_{18}$. *Lithos* **1**, 275-285.
- HAWTHORNE, F.C. & ČERNÝ, P. (1977): The alkali-metal positions in Cs-Li beryl. *Can. Mineral.* **15**, 414-421.
- _____ & GROAT, L.A. (1985): The crystal structure of wroewolfeite, a mineral with $\text{Cu}_4(\text{OH})_6(\text{SO}_4)(\text{H}_2\text{O})$ sheets. *Am. Mineral.* **70**, 1050-1055.
- _____ & SMITH, J.V. (1986): Enumeration of 4-connected 3-dimensional nets and classification of framework silicates. 3D nets based on insertion of 2-connected vertices into 3-connected plane nets. *Z. Kristallogr.* **175**, 15-30.
- MANIER-GLAVINAZ, V., COUTY, R. & LAGACHE, M. (1989b): The removal of alkalis from beryl: structural adjustments. *Can. Mineral.* **27**, 663-671.
- _____, D'ARCO, P. & LAGACHE, M. (1989a): Alkali partitioning between beryl and hydrothermal fluids: an experimental study at 600°C and 1.5 kbar. *Eur. J. Mineral.* **1**, 645-655.
- MOROSIN, B. (1972): Structure and thermal expansion of beryl. *Acta Crystallogr.* **B28**, 1899-1903.
- OTTAWAY, T.L., WICKS, F.J., BRYNDZIA, L.T. & SPOONER, E.T.C. (1986): Characteristics and origin of the Muzo emerald deposit, Columbia. *Int. Mineral. Assoc., 14th Gen. Meet., Abstr.*, 193.
- POUCHOU, J.L. & PICOIR, F. (1985): A new model for quantitative X-ray microanalysis. *Rech. Aerosp.* **1984-3**, 13-38.
- SHERRIFF, B.L. & GRUNDY, H.D. (1988): Calculations of ^{29}Si MAS nmr chemical shift from silicate mineral structure. *Nature* **332**, 819-822.
- _____ & _____ (1991): The relationship between ^{29}Si MAS NMR chemical shift and silicate mineral structure. *Eur. J. Mineral.* (in press).
- _____, _____ & HARTMAN, J.S. (1987): Analysis of fluid inclusions using nuclear magnetic resonance. *Geochim. Cosmochim. Acta* **51**, 2233-2235.
- TARTE, P. (1964): Identification of Li-O bands in the infra-red spectra of simple lithium compounds containing LiO_4 tetrahedra. *Spectrochim. Acta* **20**, 238-240.
- ZOLTAI, T. (1960): Classification of silicates and other minerals with tetrahedral structures. *Am. Mineral.* **45**, 960-973.

Received September 15, 1990, revised manuscript accepted January 7, 1991.